Results in Physics 8 (2018) 516–523

Contents lists available at ScienceDirect

Results in Physics

journal homepage: www.journals.elsevier.com/results-in-physics

On steady two-dimensional Carreau fluid flow over a wedge in the presence of infinite shear rate viscosity

Masood Khan, Humara Sardar *

Department of Mathematics, Quaid-i-Azam University, Islamabad 44000, Pakistan

ARTICLE INFO

Article history:
Received 2 November 2017
Received in revised form 22 November 2017
Accepted 25 November 2017
Available online 20 December 2017

Keywords:
Static/moving wedge
Carreau viscosity model
Heat transfer analysis
Numerical computations

ABSTRACT

This paper investigates the steady two-dimensional flow over a moving/static wedge in a Carreau viscosity model with infinite shear rate viscosity. Additionally, heat transfer analysis is performed. Using suitable transformations, nonlinear partial differential equations are transformed into ordinary differential equations and solved numerically using the Runge–Kutta Fehlberg method coupled with the shooting technique. The effects of various physical parameters on the velocity and temperature distributions are displayed graphically and discussed qualitatively. A comparison with the earlier reported results has been made with an excellent agreement. It is important to note that the increasing values of the wedge angle parameter enhance the fluid velocity while the opposite trend is observed for the temperature field for both shear thinning and thickening fluids. Generally, our results reveal that the velocity and temperature distributions are marginally influenced by the viscosity ratio parameter. Further, it is noted that augmented values of viscosity ratio parameter thin the momentum and thermal boundary layer thickness in shear thickening fluid and reverse is true for shear thinning fluid. Moreover, it is noticed that the velocity in case of moving wedge is higher than static wedge.

Introduction

Quite recently researchers have shown their keen interest in the study of fluid flow across the wedge formed figures. It has a vital importance in the fields of geothermal industries, aerodynamics, enhanced oil recovery, heat exchangers and geothermal systems, etc. Historically, a numerous literature on Falkner and Skan flow over a static wedge can be found in the books of Gersten and Schlichting [1] and Leal [2]. In the last few years, experts have taking much interest in the Falkner-Skan flow by considering the impacts of numerous parameters. The solutions and their dependence on β (the wedge angle) were latterly examined by Hartree [3]. He developed the solutions and velocity profile for different approximations of pressure gradient parameter.

The influence of suction/injection on forced convective wedge flow with uniform heat flux was examined by Yih [4]. His numerical study cast out that the flow separation only happens for the pressure gradient parameter $m = 0$. Ishaq et al. [5] discussed the steady 2D magnetohydrodynamic wedge flow of micropolar fluid in the presence of variable wall temperature. The boundary layer flows including variety of non-Newtonian fluids over stretching surfaces have received extensive attention in the literature. Some later works on the boundary layer flow of non-Newtonian fluids are offered in [6–9]. However, many fluids are non-Newtonian in their flow features and are suggested as rheological fluid models. Non-Newtonian fluids have a much utilization in engineering than Newtonian fluids. Examples are crystal growth, pharmaceuticals, products of everyday sustenance, fiber innovation and so on.

Ellahi et al. [10] examined the Numerical study of magnetohydrodynamics generalized Couette flow of Eyring-Powell fluid with heat transfer and slip condition. The study of Falkner-Skan flow of Carreau fluid over a wedge in the presence of crossed diffusion and magnetic field was investigated by Raju and Sandeep [11]. An analysis on MHD Falkner-Skan flow of Casson fluid past a wedge was also performed by Raju and Sandeep [12]. Khan and Azam [13] discussed the unsteady heat and mass transfer mechanisms in MHD Carreau nanofluid flow. Further, Khan and Azam [14] studied the unsteady Falkner-Skan flow of MHD Carreau nanofluid past a static/moving wedge with convective surface condition. Rajagopal et al. [15] discussed the Falkner-Skan flows of a non-Newtonian fluid. Kuo [16] discussed the application of the differential transformation method to the solutions of Falkner-Skan wedge flow. Recently, Khan and Hashim [17] explored the boundary layer flow

* Corresponding author.
E-mail address: humarasardar@math.qau.edu.pk (H. Sardar).

https://doi.org/10.1016/j.rinp.2017.11.039
2211-3797/

and heat transfer to Carreau fluid over a nonlinear stretching sheet. Additionally Khan and Hashim [18] investigated the impact of heat transfer on Carreau fluid flow past a static/moving wedge. Few studies associated with non-Newtonian model can be seen in [19–29].

The present study is aimed at analyzing the heat transfer analysis in Carreau viscosity fluid model past a static/moving wedge with infinite shear rate viscosity. It is important to note that Carreau fluid is a distinct class of generalized Newtonian fluid which classifies shear thinning and shear thickening nature of fluids. The governing partial differential equations system is reduced to a set of non-linear ordinary differential equation by applying suitable transformations. Later, they are solved numerically using Runge–Kutta fourth-fifth order method along with shooting technique. The influences of the pertinent flow variables are described through graphs and tables.

Mathematical formulation

Here we have considered the laminar, steady two-dimensional flow of an incompressible Carreau viscosity fluid model past a static/moving wedge as shown through Fig. 1. We supposed that fluid flow is induced by the stretching wedge with velocity $u_w(x) = bx^m$ while the free stream velocity is $u_e(x) = ax^m$, where a, b, c and $m$are positive constants. Further $u_w(x) > 0$ shows the stretching wedge surface velocity and $u_w(x) < 0$ compares to contracting wedge surface velocity.

The wedge angle is assumed to be $\Omega = \beta\pi$, where $\beta = \frac{2m}{m+1}$ is related to the pressure gradient. It is anticipated that the surface temperature $T_w(x)$ at the sheet considered to be higher than the ambient fluid temperature T_∞ $(T_w > T_\infty)$. The constitutive equations for the generalized Newtonian Carreau viscosity model [14,17] are given as

$$\boldsymbol{\tau} = -p\mathbf{I} + \mu(\dot{\gamma})\mathbf{A}_1, \quad \mu = \mu_\infty + (\mu_0 - \mu_\infty)\left[1 + (\Gamma\dot{\gamma})^2\right]^{\frac{n-1}{2}}, \tag{1}$$

$$\dot{\gamma} = \sqrt{\frac{1}{2}\Pi} = \sqrt{\frac{1}{2}trace\left(\mathbf{A}_1^2\right)}. \tag{2}$$

The apparent viscosity μ of Carreau model can also be expressed as

$$\mu = \mu_0\left[\beta^* + (1-\beta^*)[1 + (\Gamma\dot{\gamma})^2]^{\frac{n-1}{2}}\right]. \tag{3}$$

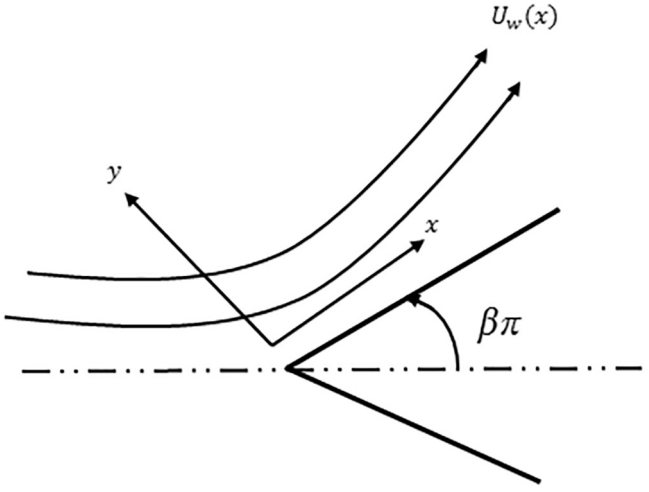

Fig. 1. Geometry of the problem.

In the above equations, $\mathbf{I}$ the identity tensor, p is the pressure, $\mathbf{A}_1 = (\text{grad}\mathbf{V}) + (\text{grad}\mathbf{V})^T$ is the first Rivlin-Erickson tensor, n the power law index, Γ a material time constant and $\beta^* = \left(\frac{\mu_\infty}{\mu_0}\right)$ the viscosity ratio parameter with μ_0 the zero shear rate viscosity and μ_∞ the infinite shear rate viscosity and chosen to be less than one in present study.

For the steady two-dimensional flow, the velocity and temperature fields are supposed to be of the form

$$V = [u(x,y), v(x,y), 0], \quad T = T(x,y), \tag{4}$$

where u and v represent the velocity components in the x- and y-directions, respectively.

On the basis of above assumptions and usual boundary layer approximations, the convective transport model for the Carreau fluid is governed by the equations of mass, momentum and energy as:

$$\frac{\partial u}{\partial x} + \frac{\partial v}{\partial y} = 0, \tag{5}$$

$$u\frac{\partial u}{\partial x} + v\frac{\partial u}{\partial y} = u_e\frac{du_e}{dx} + \nu\left(\frac{\partial^2 u}{\partial y^2}\right)\left[\beta^* + (1-\beta^*)\left\{1 + \Gamma^2\left(\frac{\partial u}{\partial y}\right)^2\right\}^{\frac{n-1}{2}}\right] + \nu(n-1)(1-\beta^*)\Gamma^2\left(\frac{\partial^2 u}{\partial y^2}\right)\left(\frac{\partial u}{\partial y}\right)^2\left\{1 + \Gamma^2\left(\frac{\partial u}{\partial y}\right)^2\right\}^{\frac{n-3}{2}}, \tag{6}$$

$$u\frac{\partial T}{\partial x} + v\frac{\partial T}{\partial y} = \alpha\frac{\partial^2 T}{\partial y^2}, \tag{7}$$

where ν is the kinematic viscosity, $\alpha = \frac{k}{\rho c_p}$ the thermal diffusivity with c_p the specific heat, k the thermal conductivity and T the temperature of the fluid.

The related boundary conditions for the present problem are:

(1) static wedge

$$u = 0, v = 0, T = T_w \quad \text{at} \quad y = 0, \tag{8}$$

$$u = u_e(x) = cx^m, T \to T_\infty \quad \text{as} \quad y \to \infty, \tag{9}$$

(2) moving wedge

$$u = u_w(x) = bx^m, \quad v = 0, T = T_w \quad \text{at} \quad y = 0, \tag{10}$$

$$u = u_e(x) = cx^m, \quad T \to T_\infty \quad \text{as} \quad y \to \infty. \tag{11}$$

Now we introduced the following suitable transformations:

$$\eta = y\sqrt{\frac{c(m+1)}{2\nu}}x^{\frac{m-1}{2}}, \quad \Psi(x,y) = \sqrt{\frac{2\nu c}{m+1}}x^{\frac{m+1}{2}}f(\eta), \quad \theta(\eta) = \frac{T - T_\infty}{T_w - T_\infty}, \tag{12}$$

where Ψ denotes stream function that satisfies equation of continuity with $u = \frac{\partial\Psi}{\partial y}$ and $v = -\frac{\partial\Psi}{\partial x}$.

Thus the transformed non-linear momentum and energy equations can be described as:

$$\left[\beta^* + (1-\beta^*)\left\{1 + We^2(f'')^2\right\}^{\frac{n-3}{2}}\left\{1 + nWe^2(f'')^2\right\}\right]f''' + ff'' + \beta\left[1 - (f')^2\right] = 0, \tag{13}$$

$$\theta'' + \Pr f\theta' = 0, \tag{14}$$

with BC,s

$$f(0) = 0, \quad f'(0) = \lambda, \quad \theta(0) = 1, \tag{15}$$

$$f'(\infty) \to 1, \qquad \theta(\infty) \to 0. \tag{16}$$

In the above equations, prime denotes the differentiation with respect to variable η, We the local Weissenberg number, β the wedge angle parameter, λ the velocity ratio parameter and Pr the Prandtl number. These quantities are defined as follows:

$$We^2 = \left(\frac{c^3\Gamma^2 x^{3m-1}}{2\nu}\right), \qquad Pr = \frac{\mu c_p}{k}, \qquad \lambda = \frac{b}{c}. \tag{17}$$

Here positive values of β show the favorable pressure gradient and negative values of β reveal an opposing pressure gradient. Additionally, $m = 0$ $(\beta = 0)$ implies the fluid flow past a flat plate and $m = 1(\beta = 1)$ means the stagnation point flow. Moreover the constant velocity ratio parameter $\lambda > 0$ and $\lambda < 0$ classify with a moving wedge in the same and opposite directions to the free stream, respectively, however, $\lambda = 0$ is related to a static wedge.

The parameters of engineering interest in the flow and heat transfer problem are the local skin friction coefficient C_{fx} and the local Nusselt number Nu_x, characterizing the surface drag and wall heat transfer rate, can be defined as:

$$C_{fx} = \frac{\tau_w}{\rho U_w^2(x)/2}, \qquad Nu_x = \frac{xq_w}{k(T_w - T_\infty)}, \tag{18}$$

where τ_w is the surface shear stress and q_w the surface heat flux given by

$$\tau_w = \mu_0\left(\frac{\partial u}{\partial y}\right)\left[\beta^* + (1-\beta^*)\left\{1 + \Gamma^2\left(\frac{\partial u}{\partial y}\right)^2\right\}^{\frac{n-1}{2}}\right], \quad q_w = -k\left(\frac{\partial T}{\partial y}\right). \tag{19}$$

Upon using Eq. (12), the local skin friction coefficient and local Nusselt number become

$$\mathrm{Re}^{1/2}C_{fx} = \frac{2}{\sqrt{2-\beta}}f''(0)\left[\beta^* + (1-\beta^*)\left\{1 + We^2(f''(0))^2\right\}^{\frac{n-1}{2}}\right],$$
$$\mathrm{Re}^{-1/2}Nu_x = -\frac{2}{\sqrt{2-\beta}}\theta'(0). \tag{20}$$

where $\mathrm{Re}_x = \frac{xu_e}{\nu}$ is the local Reynolds number.

Table 1
Contrast values of $-f''(0)$ for different β when $\beta^* = We = 0$ and $n = 1$.

β	Rajagopal et al. [16]	Kuo [17]	Present study
0	–	0.469600	0.469600
0.3	0.474755	0.775524	0.474755
0.6	0.995836	0.995757	0.995836
1.2	1.335722	1.333833	1.335722

Solution methodology

The system of governing equations (Eqs. (13) and (14)) is highly nonlinear and partially set of coupled ordinary differential equations. To discover the solution of this system along with

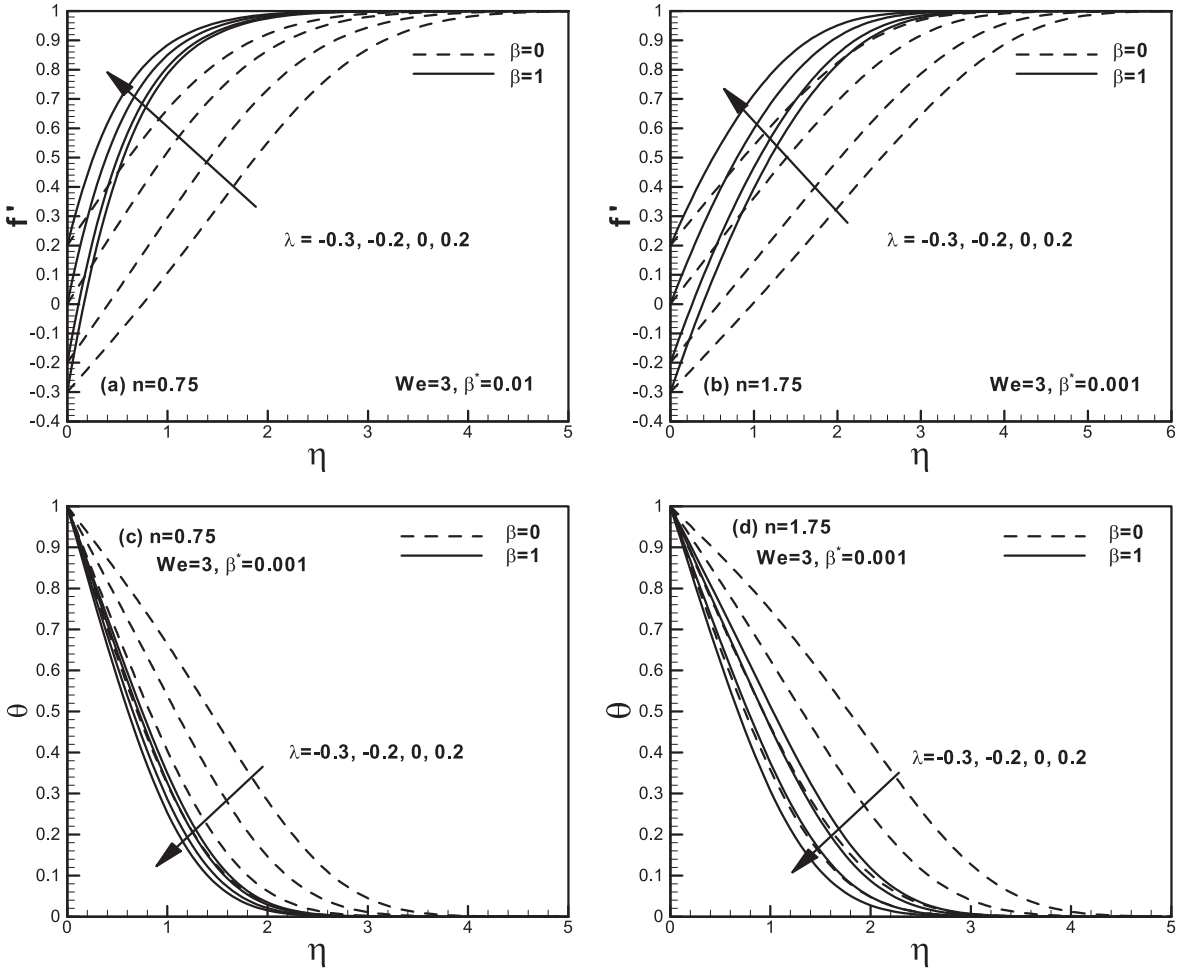

Fig. 2. Effects of the velocity ratio parameter λ on the velocity and temperature distributions.

boundary conditions (15) and (16), the shooting technique along with fourth-fifth order Runge–Kutta integration scheme is developed. Since Runge–Kutta Fehlberg method solves only initial value problem, and so Eqs. (13) and (14) are converted into set of first order equations. For this purpose, we rewrite the above set of equations as given below:

$$f''' = \frac{-\beta\left(1-(f')^2\right) - ff''}{\left[\beta^* + (1-\beta^*)\left\{1+nWe^2(f'')^2\right\}\left\{1+We^2(f'')^2\right\}^{\frac{n-3}{2}}\right]}, \tag{21}$$

$$\theta'' = -\Pr f\theta'. \tag{22}$$

The new variables defined below are employed to reduce above higher order equations into system of first order differential equations:

$$\begin{aligned} f &= y_1, \quad f' = y_2, \quad f'' = y_3, \quad f''' = y_3', \\ \theta &= y_4, \quad \theta' = y_5, \quad \theta'' = y_5'. \end{aligned} \tag{23}$$

After inserting Eq. (23) into Eqs. (13) and (14), a new system of ordinary differential equations is obtained as:

$$y_1' = y_2, y_2' = y_3, y_3' = \frac{\left[-\beta(1-y_2^2) - y_1y_3\right]}{\beta^* + (1-\beta^*)\left[1+nWe^2y_3^2\right]\left[1+We^2y_3^2\right]^{\frac{n-3}{2}}}, \tag{24}$$

$$y_4' = y_5, y_5' = -\Pr y_1y_5. \tag{25}$$

together with the boundary conditions

$$\begin{pmatrix} y_1 \\ y_2 \\ y_3 \\ y_4 \\ y_5 \end{pmatrix} = \begin{pmatrix} 0 \\ \lambda \\ u_1 \\ 1 \\ u_2 \end{pmatrix}. \tag{26}$$

Here u_1 and u_2 are the initial guesses for the values of $f''(0)$ and $\theta'(0)$.

Above system of equations is solved with shooting method, the following procedure is utilized:

1. Firstly chose the limit of η_∞ the best suited limit for η_∞ is between 5 and 10.
2. Then select suitable initial guesses for $y_3(0)$ and $y_5(0)$. Initially $y_3(0) = -1$ and $y_5(0) = 0.5$ are selected.
3. Then set of ODEs are solved with the fourth-fifth order Runge–Kutta Fehlberg scheme.
4. Finally, boundary residuals (absolute variations in given and calculated values of $y_2(\infty)$ and $y_5(\infty)$ is calculated. The solution will converge if entire values of boundary residuals are less then tolerance error, which is considered 10^{-5}.
5. If values of boundary residuals are larger than tolerance error, then values of $y_3(0)$ and $y_5(0)$ will be modified by Newton's method.

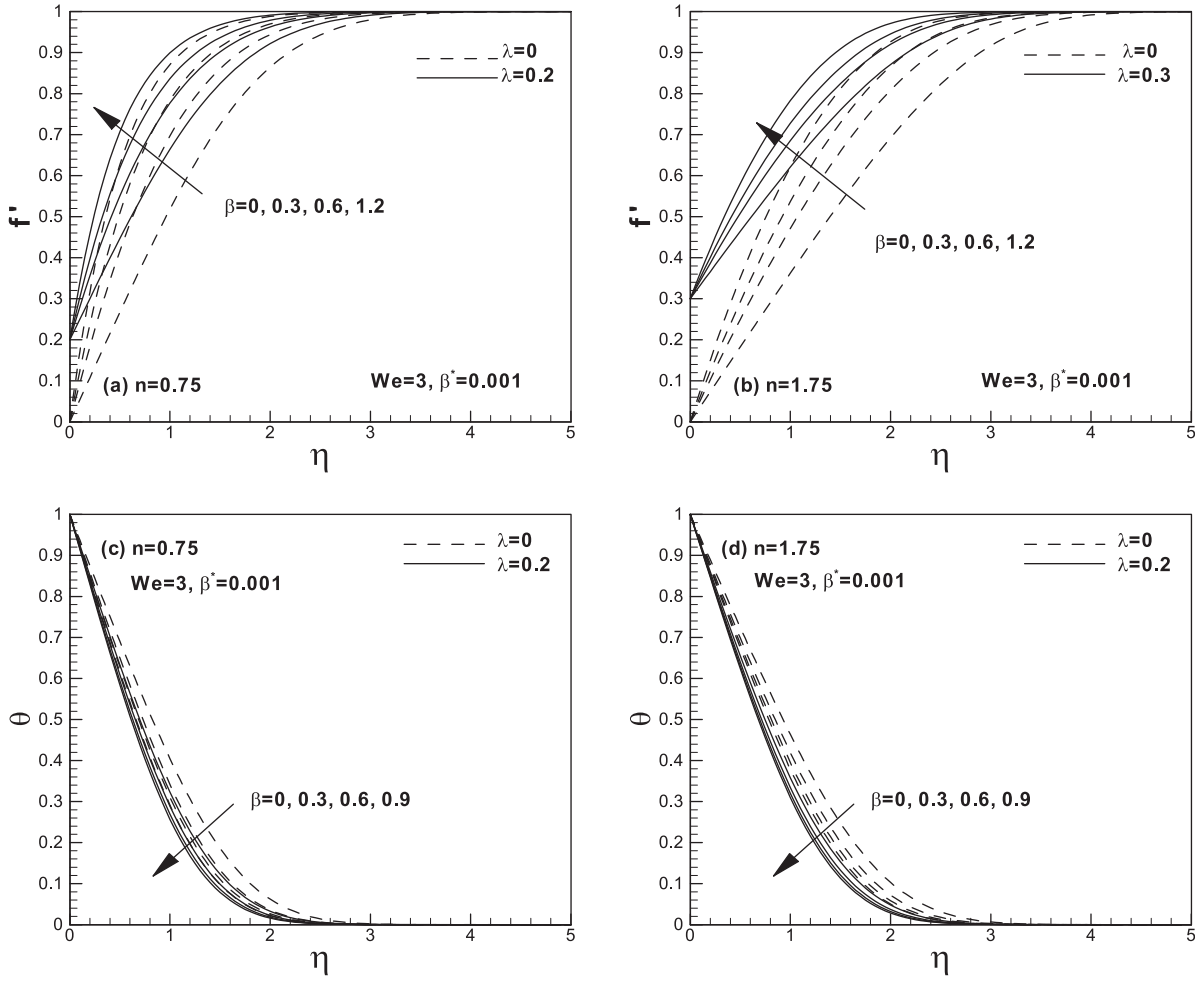

Fig. 3. Effects of the wedge angle parameter β on the velocity and temperature distributions.

Result and discussion

In order to examine results of the present problem a numerical computation is performed for steady two dimensional flow of Carreau viscosity model generated by a static/moving wedge. The partially coupled set of Eqs. (13) and (14) with boundary conditions (15) and (16) are solved numerically using Runge–Kutta fourth-fifth order method along with shooting technique. Moreover, representative results for the skin friction and local Nusselt number are recorded through tables. The influence of non-dimensional parameters like $We, \lambda, n, \beta, \beta^*$ and Pr on dimensionless fluid velocity and temperature distribution are determined and presented through graphs. Additionally the accuracy of our numerical results is verified with earlier published results by Rajgopal et al. [16] and Kuo [17] for particular cases presented in Table 1. The good agreement is reported between these results.

Fig. 2 are plotted to examine the influence of velocity ratio parameter λ on temperature $\theta(\eta)$ and velocity $f'(\eta)$ profiles, for both shear thickening $(n > 1)$ and shear thinning $(n < 1)$ fluids. Here temperature and velocity profiles are presented for two different values of β, in detail, $\beta = 0$ means wedge angle of zero degree relates to the flow over a flat plate and $\beta = 1$ relates the wedge point of 90°, i.e, stagnation point flow. From Fig. 2(a, b), we observed that the fluid velocity is enhanced by uplifting values of the velocity ratio parameter for both cases. Also it is observed that when flow is near the stagnation-point, the velocity profiles are closer to each other. However, these Figs. show that the thickness of the momentum boundary layer for shear thickening fluid is higher as compared with shear thinning fluid. Fig. 2(c, d) depict that by increasing values of the velocity ratio parameter, temperature profile decreases in both cases, i.e., for shear thinning as well as shear thickening fluids. The thermal boundary layer thickness reduces for both the flow over flat plate and near the stagnation-point. However, the temperature profiles are closer to each other if flow is near to the stagnation-point and the thermal boundary layer thickness is higher for shear thickening fluid.

Fig. 3 are designed to observe the effects of the wedge angle parameter β on the velocity $f'(\eta)$ and temperature $\theta(\eta)$ profiles in shear thinning and shear thickening fluids. From Fig. 3(a, b) we observed that the fluid velocity is enhanced by increasing wedge angle parameter in both cases. Physically it is due to the wedge angle parameter that is related with pressure gradient. Thus, positive values of the wedge angle parameter indicate a favorable pressure gradient which enhance the flow. Further for positive values of β the velocity profile goes nearer to the surface of the wedge, and opposite flow does not occur. Moreover, the momentum boundary layer thickness reduces by increasing wedge angle parameter and then again it is higher in case of shear thickening fluid. Fig. 3(c, d) describe the impact of the wedge angle parameter on thermal boundary layer. We observed that the fluid

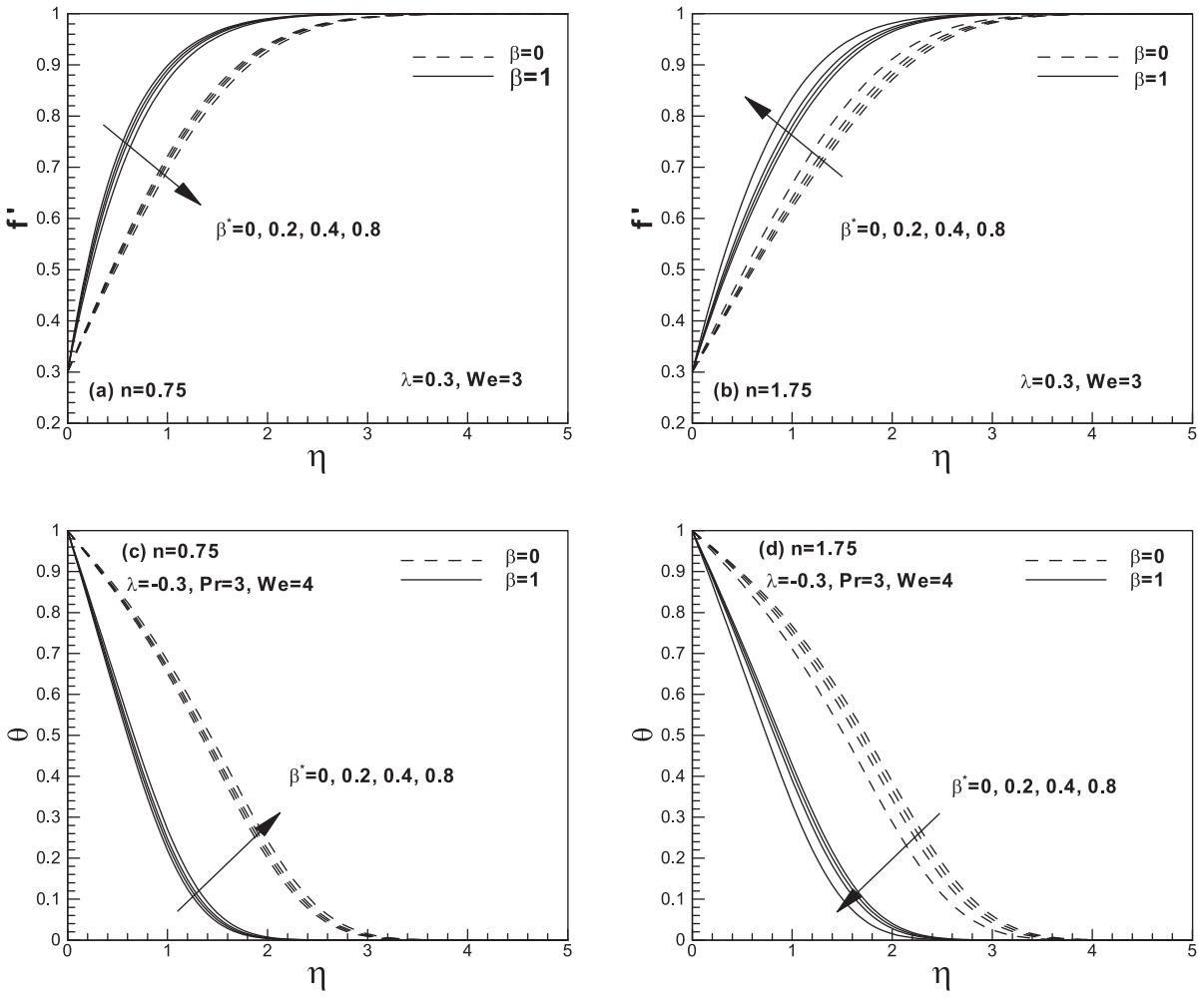

Fig. 4. Effects of the viscosity ratio parameter β^* on the velocity and temperature distribution for different wedge angle parameter.

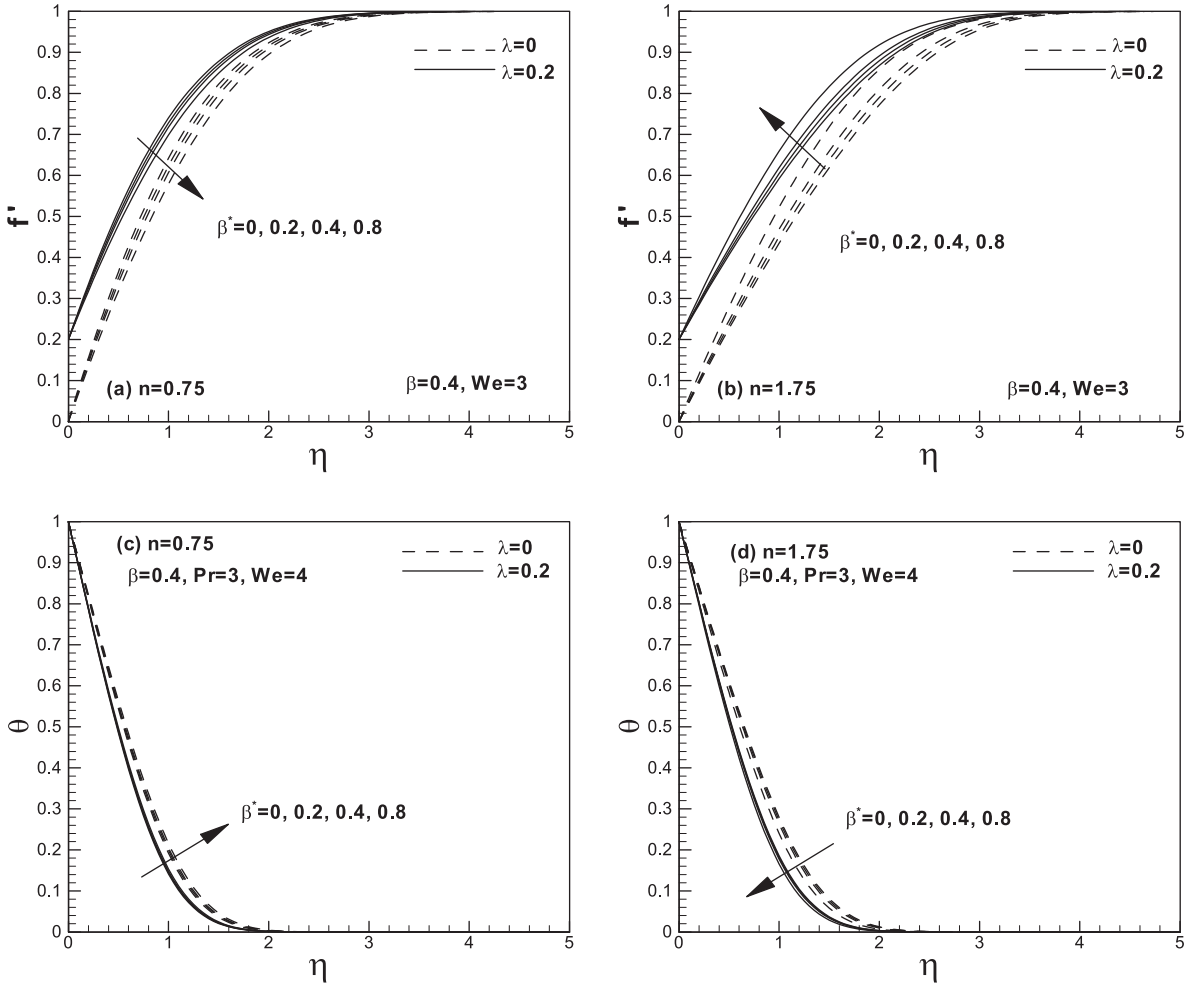

Fig. 5. Effects of the viscosity ratio parameter β^* on the velocity and temperature distributions.

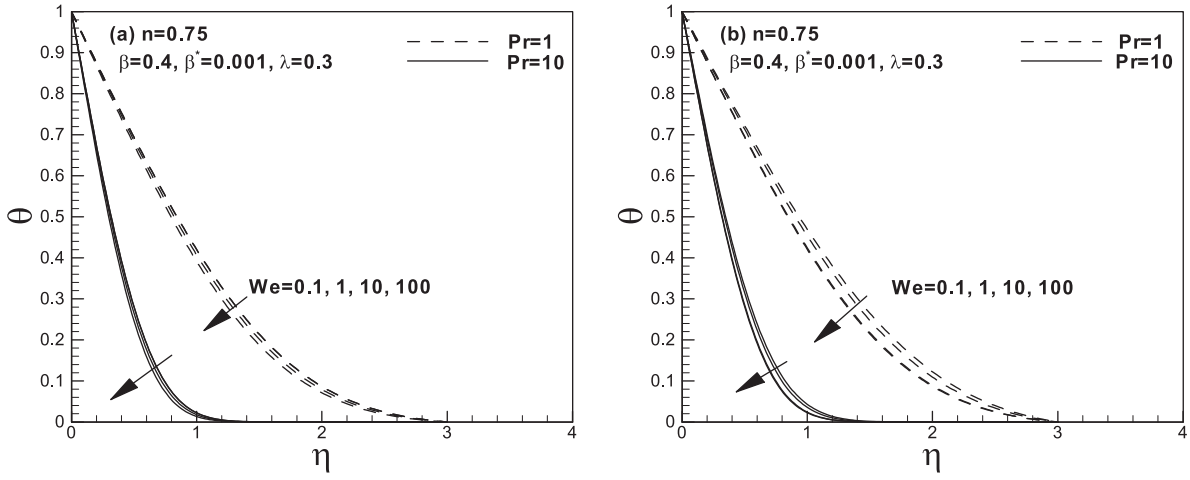

Fig. 6. Effects of the Weissenberg number *We* on the temperature distribution.

temperature is diminished with increasing the wedge angle parameter. Moreover, the maximum temperature of the fluid occur for the flow over flat plate ($\beta = 0$). Physically, it is due to the fluid motion i.e., pressure gradient is zero and due to that fluid temperature increases at the surface of wedge. In the case of static wedge the thermal boundary layer thickness is higher.

Fig. 4 describe the impact of viscosity ratio parameter β^* on velocity and temperature profiles for both shear thinning and thickening cases. Here profiles are presented for two different values of wedge angle parameter. Here $\beta = 0$ (wedge of zero degree) and $\beta = 1$ (wedge point of 90°). We observe a minor dependence of velocity and temperature distributions on β^*. However, it is

interesting to note that graph of velocity and temperature disclose quite the opposite trends with uplifting β^* for the shear thinning and shear thickening fluids. Additionally, these Figs. portray that the momentum and thermal layers thickness become thick in shear thinning fluid as we increase the viscosity ratio parameter and quite the opposite is true for shear thickening fluid. Fig. 5 show the impact of viscosity ratio parameter β^* on the velocity and temperature profiles for both shear thinning and thickening cases with two different values of λ. Here $\lambda = 0$ (static wedge) and $\lambda > 0$ and $\lambda < 0$ show the moving wedge in same and inverse directions, respectively. We observe again a little dependence of the velocity and temperature distributions on β^*. Qualitatively, the effects of β^* on the velocity and temperature distributions are same as that of Fig. 4.

Fig. 6 is a plot of the variation in the temperature distribution for various values of the Weissenberg number *We* and Prandtl number *Pr* for both shear thinning and shear thickening fluids. These Figs. exhibit that the temperature and thermal boundary layer thickness reduce by uplifting the values of *We* and *Pr* in both shear thinning and shear thickening fluids. Moreover, it can be observed that the maximum difference between the temperature profiles occurs at smaller values of *Pr* and it reduces as *Pr* increases.

Table 1 is created to prove the authenticity of the given numerical results with the previous published data for shear thinning $(n < 1)$ and shear thickening $(n > 1)$ fluids and found to be in outstanding agreement. Table 2 provides numerical results of the local Nusselt number $Re^{-1/2}\ Nu_x$ for selected values of viscosity ratio parameter (β^*), wedge angle parameter (β) and velocity ratio parameter (λ) for both shear thinning $(n < 1)$ and shear thickening $(n > 1)$ cases.

Table 2 is created to exhibit the influence of the viscosity ratio parameter β^*, velocity ratio parameter λ and wedge angle parameter β on the local skin friction coefficient for both shear thinning and thickening cases. On the basis of this table it is noticed that the local skin friction coefficient is decreasing function for the wedge angle parameter and velocity ratio parameter in both cases. It is also observed that the local skin friction coefficient is a decreasing function for the viscosity ratio parameter in shear thinning case and reverse is true for shear thickening case.

Table 3 is constructed to depict the impact of the viscosity ratio parameter β^*, velocity ratio parameter λ and wedge angle parameter β on the local Nusselt number for both cases when $Pr = 1$ and $We = 3$. It is observed that the local Nusselt number is a decreasing function for velocity ratio parameter and viscosity ratio parameter in both shear thinning and shear thickening cases. It is further discovered that the local Nusselt number increasing function for the viscosity ratio parameter in shear thinning case and reverse is true for shear thickening case.

Table 2
Numerical values of the skin friction coefficient $Re^{1/2}C_{fx}$ for different β^*, β and λ when Pr = 1 and $We = 3$.

β^*	β	λ	$Re^{1/2}C_{fx}$	
			$n = 0.75$	$n = 1.75$
0	0.3	0.2	0.961012	1.22977
0.2			0.979278	1.20104
0.4			0.996203	1.16925
0.8			1.026900	1.09174
0.001	0	0.2	0.594385	0.706434
	0.3		0.961107	1.22963
	0.6		1.310680	1.77143
	1.2		2.23300	3.26384
0.001	0.3	−0.3	1.170530	1.56324
		−0.2	1.157030	1.54768
		0	1.084620	1.43226
		0.2	0.961107	1.22963

Table 3
Numerical values of the local Nusselt number $Re^{-1/2}Nu_x$ for different β^*, β and λ when Pr = 1 and $We = 3$.

β^*	β	λ	$Re^{-1/2}Nu_x$	
			$n = 0.75$	$n = 1.75$
0	0.3	0.2	0.916605	0.860677
0.2			0.912067	0.865626
0.4			0.90800	0.871354
0.8			0.900932	0.886604
0.001	0	0.2	0.795146	0.758852
	0.3		0.916581	0.860700
	0.6		1.04584	0.973570
	1.2		1.44201	1.33020
0.001	0.3	−0.3	0.664451	0.529774
		−0.2	0.722834	0.605179
		0	0.825856	0.740896
		0.2	0.916581	0.860700

Conclusions

In this article numerical computations for steady 2D Carreau fluid flow over a static/moving wedge with infinite shear rate viscosity have been performed. Boundary layer equations for steady 2D Carreau fluid flow were derived in the presence of infinite shear rate viscosity. For numerical calculations we have utilized R-K Fhelberg fourth-fifth order method alongside with shooting technique. The current numerical calculations were compared with the available results in the literature with outstanding agreement. The following decision can be drawn from the above numerical calculations.

- By increasing the wedge angle parameter β, a reduction was observed in the momentum and thermal boundary layer thicknesses.
- Increasing the velocity ratio parameter λ, velocity profile was increased and opposite trend was observed in temperature profile.
- The velocity distribution was decreased for shear thinning fluid and increased for shear thickening fluid by increasing viscosity ratio parameter for both static/moving wedge and quite the opposite was true for temperature distribution.
- The momentum and thermal boundary layers thicknesses were higher for shear thickening fluid when compared with shear thinning fluid.

Conflict of interest

The authors declare that they have no conflict of interest.

References

[1] Schlichting H, Gersten K. Boundary Layer Theory. Berlin: Springer-Verlag; 2000.
[2] Leal LG. Advanced transport phenomena: fluid mechanics and convective transport processes. New York: Cambridge University Press; 2007.
[3] Hartree DR. On an equation occurring in Falkner and Skan's approximate treatment of the equations of the boundary layer. Proc Camb Philos Soc 1937;33:223–39.
[4] Yih KA. Uniform suction/blowing effect on forced convection about a wedge: uniform heat flux. Acta Mech 1998;128:173–81.
[5] Ishaq A, Nazar R, Pop I. MHD Boundary-layer flow of a micropolar fluid past a wedge with variable wall temperature. Acta Mech 2008;196:75–86.
[6] Hayat T, Sajjad R, Muhammad T, Alsaedi A, Ellahi R. On MHD nonlinear stretching flow of Powell-Eyring nanomaterial. Res Phys 2017;7:535–43.
[7] Hayat T, Sajjad R, Ellahi R, Muhammad T, Ahmad B. Numerical study of boundary-layer flow due to a nonlinear curved stretching sheet with convective heat and mass conditions. Res Phys 2017;7:2601–6.
[8] Sajjad R, Hayat T, Ellahi R, Muhammad T, Alsaedi A. Stagnation-point flow of second grade nanofluid towards a nonlinear stretching surface with variable thickness. Res Phys 2017;7:2821–30.
[9] Hayat T, Sajjad R, Ellahi R, Muhammad T, Ahmad B. Numerical study for Darcy-Forchheimer flow due to a curved stretching surface with Cattaneo-Christov heat flux and homogeneous-heterogeneous reactions. Res Phys 2017;7:2886–92.

[10] Ellahi R, Shivanian E, Abbasbandy S, Hayat T. Numerical study of magnetohydrodynamics generalized Couette flow of Eyring-Powell fluid with heat transfer and slip condition. Int J Numer Math Heat Fluid Flow 2016;26(5):1433–45.
[11] Raju CSK, Sandeep N. Falkner-Skan flow of a magnetic-Carreau fluid past a wedge in the presence of cross diffusion effects. Eur Phys J Plus 2016;131:267.
[12] Raju CSK, Sandeep N. Nonlinear radiative magnetohydrodynamic Falkner-Skan flow of Casson fluid over a wedge. Alex Eng J 2016;55:2045–54.
[13] Khan M, Azam M. Unsteady heat and mass transfer mechanisms in MHD Carreau nano fuid flow. J Mol Liq 2017;225:554–62.
[14] Khan M, Azam M. On unsteady Falkner-Skan flow of MHD Carreau nanofluid past a static/moving wedge with convective surface condition. J Mol Liq 2017;230:48–58.
[15] Rajagopal KR, Gupta AS, Na TY. A note on the Falkner-Skan flows of a non-Newtonian fluid. Int J Non Linear Mech 1982;18(4):313–20.
[16] Kuo BL. Application of the differential transformation method to the solutions of Falkner-Skan wedge flow. Acta Mech 2003;164:161–74.
[17] Khan M, Hashim. Boundary layer flow and heat transfer to Carreau fluid over a nonlinear stretching sheet. AIP Adv 2016;5:101203.
[18] Khan M, Hashim. Impact of heat transfer analysis on Carreau fluid flow past a static/moving wedge. Therm Sci 2016:169.
[19] Khan WA, Khan M, Alshomrani AS, Ahmad L. Numerical investigation of generalized Fourier's and Fick's laws for Sisko fluid flow. J Mol Liq 2016;224:1016–21.
[20] Khan WA, Khan M, Irfan M, Alshomrani AS. Impact of melting heat transfer and nonlinear radiative heat flux mechanisms for the generalized Burgers fluids. Res Phys 2017;7:4025–32.
[21] Khan WA, Khan M. Impact of thermophoresis particle deposition on three-dimensional radiative flow of Burgers fluid. Res Phys 2016;6:829–36.
[22] Muhammad N, Nadeem S, Haq R Ul. Heat transport phenomenon in the ferromagnetic fluid over a stretching sheet with thermal stratification. Res Phys 2017;7:854–61.
[23] Haq R, Rashid I, Khan ZH. Effects of aligned magnetic field and CNTs in two different base fluids over a moving slip surface. J Mol Liq 2017;243:682–8.
[24] Rehman S, Haq R, Khan ZH, Lee C. Entropy generation analysis for non-Newtonian nanofluid with zero normal flux of nanoparticles at the stretching surface. J Taiwan Inst Chem Eng 2016;63:226–35.
[25] Shirvan KM, Mamourian M, Mirzakhanlari S, Ellahi R. Two phase simulation and sensitivity analysis of effective parameters on combined heat transfer and pressure drop in a solar heat exchanger filled with nanofluid by RSM. J Mol Liq 2016;220:888–901.
[26] Shirvan KM, Ellahi R, Mirzakhanlari S, Mamourian M. Enhancement of heat transfer and heat exchanger effectiveness in a double pipe heat exchanger filled with porous media: numerical simulation and sensitivity analysis of turbulent fluid flow. Appl Ther Eng 2016;109:761–74.
[27] Bhatti MM, Zeeshan A, Ellahi R. Heat transfer analysis on Peristaltically induced motion of particle-fluid suspension with variable viscosity: clot blood model. Comp Meth Prog Bio 2016;137:115–24.
[28] Khan A, Khan H, Vafai K, Ellahi R. Study of peristaltic flow of magnetohydrodynamic Walter's B fluid with slip and heat transfer. Sci Iranica 2016;23(6):2650–62.
[29] Bhatti MM, Zeeshan A, Ellahi R. Electromagnetohydrodynamic (EMHD) peristaltic flow of solid particles in a third-grade fluid with heat transfer. Mech Ind 2017;18(314):1–9.